Laboratory experiments on the determination of porosity of granular soils from Ontario, Canada, using electrical resistivity measurements

Zaid Al-Qaysi and Abouzar Sadrekarimi, Ph.D., P. Eng.

Department of Civil and Environmental Engineering, Western University, London, Ontario, Canada, Tel: +1 (519) 661-2111 (Ext. 80334); Email: asadrek@uwo.ca

ABSTRACT

The difficulty of assessing soil properties such as relative density due sample disturbance and the expensive methods of obtaining undisturbed field samples of granular soils has increased the need for finding inexpensive in-situ testing methods. The approach of using geophysical techniques by measuring the electrical resistance of cohesionless soil can be used to define many geotechnical parameters and physical properties of sand without the need to obtain field samples for laboratory tests, thereby minimizing the effects of soil disturbance. This paper presents an experimental testing program for investigating the effects of pore water salinity, soil fabric, porosity, and fines content on electrical resistivity of saturated sands. The results show that the electrical resistivity of saturated sands decreases with increasing porosity, or increasing electrolyte concentration and fines content at a certain porosity, while sand fabric and gradation have relatively minor influence. Empirical correlations are thus developed for estimating sand porosity and hydraulic conductivity. The proposed correlations would be useful engineering tools to determine the in-situ porosity and seepage characteristics of sands.

Keywords: Electrical resistivity, fines content, porosity, permeability, formation factor, soil, Ontario, Canada

Introduction

Shearing strength and the mechanical behavior of saturated cohesionless soils is very important in the stability of slopes, tailings dams, bearing capacity of foundations, and the stability and design of soil retaining structures. Slope failures and landslides often results from the inadequate strength of soil compared to the applied shear stress. For example, the Merriespruit gold mine tailings dam in Virginia, South Africa was constructed by the hydraulic filling of loose mine tailings. As a result of increasing the applied shear stress by oversteepening, the tailings dam experienced slope failure followed by a massive flowslide failure in February 1994 which released 600,000 m^3 of waste tailings over a distance of more than 2,000 m, killed 17 people, and destroyed 280 houses (Fourie, et al., 2001). More recently, a catastrophic landslide occurred on the 22th of March 2014 in Oso, Washington (USA) after three weeks of intense rainfall. The Oso landslide mass obliterated more than 50 homes, claimed 43 lives, injured 10 people, and buried portions of a major state highway leading to an estimated capital loss of at least $50 million. The failure occurred in a loose sandy colluvial material susceptible to undrained shearing failure and static liquefaction (Keaton, et al., 2014). Despite considerable advances in understanding landslide mechanisms, these phenomena continue to cause significant damage throughout the world partly due to the extreme difficulties and large expenses associated with undisturbed sampling of saturated cohesionless soils for assessing their in-situ strength and determining their susceptibility to failure.

The mechanical behavior and shear strength of cohesionless soils subject to shear stress (e.g. in a laboratory triaxial shear test, beneath a slope, behind a retaining wall, or within an earth or tailings dam) are largely controlled by their density and porosity (Sadrekarimi, 2013). For example, Figure 1 illustrates the strong effect of porosity on the shearing behavior and the strength of Illinois river sand specimens in triaxial compression shear tests (Sadrekarimi, 2009). The undrained strength obtained from triaxial compression tests on soil specimens reconstituted at the in-situ porosity could then be extended to the field for assessing the stability of slopes, and the design of embankment or tailings dams. Therefore, determination of in-situ porosity and thus density of sands is essential for predicting the in-situ shearing strength and liquefaction susceptibility behavior, densification control, as well as determining seepage characteristics of cohesionless soils. These parameters at the top 10 m of a seabed are particularly important for the design of most offshore structures (e.g. oil platforms, wind turbine foundations, oil pipelines).

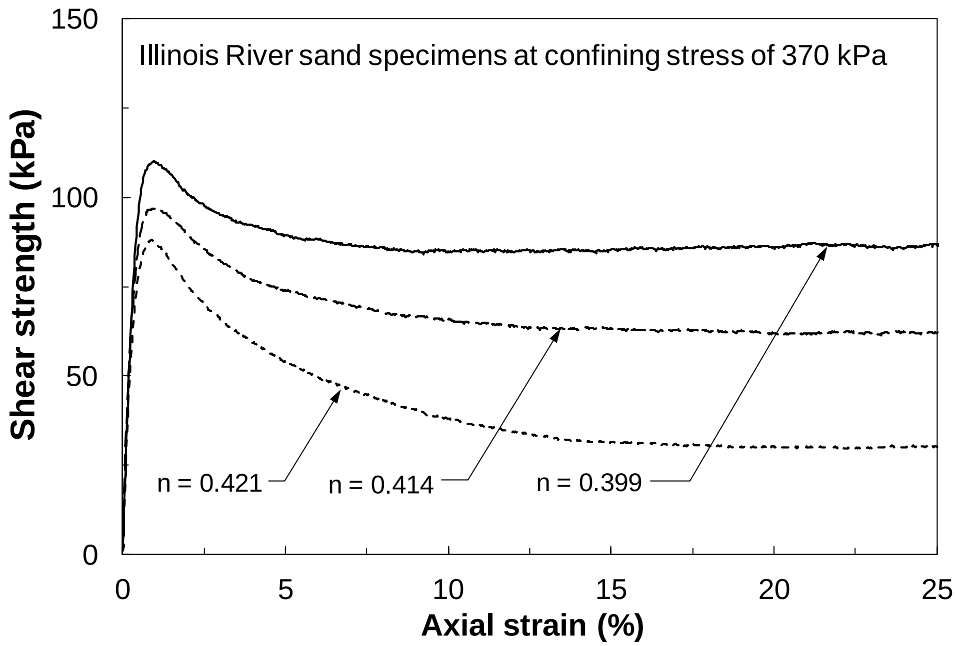

Figure 1: Effect of porosity (*n*) on the undrained shearing behavior of Illinois river sand in triaxial compression tests (Sadrekarimi, 2009)

However, direct measurement of the in-situ porosity and density of cohesionless soils is challenging due to the difficulties in obtaining undisturbed samples for laboratory testing and the susceptibility of cohesionless soil samples to disturbance caused by borehole excavation, sampling, during transportation, and sample extrusion and handling. In particular, saturated sands are notoriously difficult to sample without disturbance. Even carefully collected, thin-wall cores are likely to collapse during sampling or sample extrusion resulting in an underestimation of the in-situ porosity. This becomes further complicated by the inherent variability of field soil deposits which makes even the few high-quality undisturbed samples inadequate for characterizing subsurface soil conditions. These challenges have increased the need of finding more reliable and cost-effective in-situ testing methods. Geophysical techniques and in particular soil electrical resistivity measurements, have been used for examining the in-situ porosity (Barnes, et al., 1972, Erchul and Nacci, 1971, Jackson, et al., 1978, Kermabon, et al., 1969, Taylor-Smith, 1971, Wheatcroft, 2002) and permeability (Abu-Hassanein, et al., 1996, Jones and Buford, 1951, Kosinski and Kelly, 1981, Urish, 1981) of sediments, characterizing the degree of soil compaction (Abu-Hassanein, et al., 1996) and consolidation behavior (Bryson and Bathe, 2009, Cho, et al., 2004, Kim, et al., 2011, Lee, et al., 2008) without obtaining field samples, and thus minimize soil disturbance effects. For example, Kermabon et al. (1969) developed a field electrical resistivity probe for predicting the in-situ porosity of marine sediments, composed of interbedded clay and sand layers. Wheatcroft (2002) used an in-situ resistivity probe to measure the near-surface porosity of shallow-water marine sediments off Florida and Bahamas. The measurements indicated a thin zone of higher porosity near the surface of seabed, small-scale porosity fluctuations in the subsurface, and horizontal variation in the near-surface porosity. Cho et al. (2004) used electrical resistivity for measuring soil water content and the consolidation process of a clay soil. Lee et al. (2008) used electrical resistivity measurements for monitoring the consolidation behavior of clays and estimating the preconsolidation pressure. Bryson and Bathe (2009) developed a multi-electrode cell to measure the bulk electrical resistivity and anisotropy of compacted sand-clay soil mixtures at different volumetric water. Kim et al. (2011) developed a four-electrode resistivity probe for the measurement of porosity variation during consolidation of a mixture of kaolinite clay and crushed sand. The objective of this study is to examine relationships between electrical resistivity, permeability, and porosity of cohesionless soils and the factors affecting these relationships.

Theoretical Basis

Electrical resistivity, ρ (ohm·m) of a material is a measure of how well the material allows the flow of an electrical current through it. As particles (composed of quartz, feldspar, or carbonates) of a cohesionless soil are often non-conductive and act as insulators, the flow of an electrical current through a saturated granular soil occurs primarily through the pore water. Therefore, conductivity, volume, and the distribution of the pore water control the bulk electrical resistivity of sands (ρ_b). Accordingly, ρ_b can be directly related to the pore water resistivity (ρ_f) and pore volume (characterized by soil porosity n) using the following general empirical relationship (Archie, 1942, Winsauer, et al., 1952):

$$\frac{\rho_b}{\rho_f} = an^{-m} \qquad \text{Equation [1]}$$

where exponent *m* and coefficient *a* are fitting parameters which depend on pore volume geometry and soil particle cementation (Schon, 2004). These parameters can be determined from laboratory calibration experiments. The exponent, m varies from 1.0 – 1.5 for clean sands to 1.9 – 3.3 for clayey soils (Atkins and Smith, 1961, Barnes, et al., 1972, Campanella and Weemees, 1990, Carothers and Porter, 1971, Erchul and Nacci, 1971, Jackson, et al., 1978, Salem and Chilingarian, 1999, Taylor-Smith, 1971). The coefficient a is found to vary within 1.2 – 1.4 for loosely deposited young sands and tends to increase with increasing the density and age of a deposit (Boyce, 1968, Carothers and Porter, 1971, Erchul and Nacci, 1971, Schon, 2004). For example, Erchul and Nacci (1971) found a = 1.3 and 1.5 for loose and dense Ottawa sand samples, respectively. The ratio ρ_b/ρ_f is known as the "formation factor" (*FF*) which expresses the effects of changes in pore water resistivity as a result of the presence of non-conductive sand particles (Schon, 2004). Similar to ρ_b, *FF* is an intrinsic property of a soil which depends on the volume and the geometry of soil pore spaces.

Several investigators have found reasonable agreement between electrical resistivity and porosity measurements with Equation [1] (Erchul and Nacci, 1971, Hulbert, et al., 1982, Jackson, et al., 1978). For example, Erchul and Nacci (1971) investigated the changes in the electrical resistivity of different soil types (including an illite clay, a kaolinite clay, Providence silt, Ottawa sand with rounded particles, a glacial sand with angular particles, and a marine sediments) with varying interstitial pore water salinity. Their findings suggest that porosity can be predicted within ±2% on the basis of the formation factor measurements made in the laboratory using Equation [1]. Jackson et al. (1978) investigated unconsolidated marine sands using laboratory electrical resistivity measurements. They found that the formation factor – porosity relationship for unconsolidated marine sands was governed by Equation [1]. They also observed that the exponent m was sensitive to the shape of the particles, and it increased as the particles became angular. Erickson and Jarrard (1998) examined the relationship between porosity and electrical resistivity of shallow silica sediments from the Amazon Fan and found that muds and sands exhibit different trends of porosity and formation factor due to differences in pore volume and tortuosity. Accordingly, Equation [1] has been historically the first practical relationship between a readily measurable soil property and soil porosity (Schon, 2004).

Experimental Program

The experiments of this study were aimed to determine the effects of fines content, sand fabric, salt concentration and porosity on the electrical resistivity of sands as discussed in the following paragraphs.

Sample preparation

As illustrated in Figure 2, sand samples were prepared using undercompaction moist tamping in a cylindrical acrylic chamber with an internal diameter and height of 114.4 mm and 250 mm, respectively. The samples were then saturated by soaking them with water for 24 hours in order for the water to percolate the pore spaces among sand particles. An average degree of saturation of 96% was confirmed based on the volume and weight measurements of saturated samples. In the moist tamping method, the dry sand was premixed with 5% moisture and thoroughly mixed to uniformly distribute the moisture content. Then predetermined weights of the moist sand were deposited and tamped in 5 layers of 50 mm thick using an adjustable-height handheld tamper. The structure of specimens prepared by moist tamping resembles that of hydraulically transported sand fills. The weight of wet soil placed in the lower layers was intentionally less than those of the upper layers in order to account for the increase in soil density as a result of tamping the successive overlying layers and improve specimen uniformity. The difference in density between successive layers is defined as the undercompaction ratio (Ladd, 1978). Based on an undercompaction ratio of 10%, the density of each layer was increased linearly from the bottom to the top of the specimen. This method led to more uniform samples and repeatable test results.

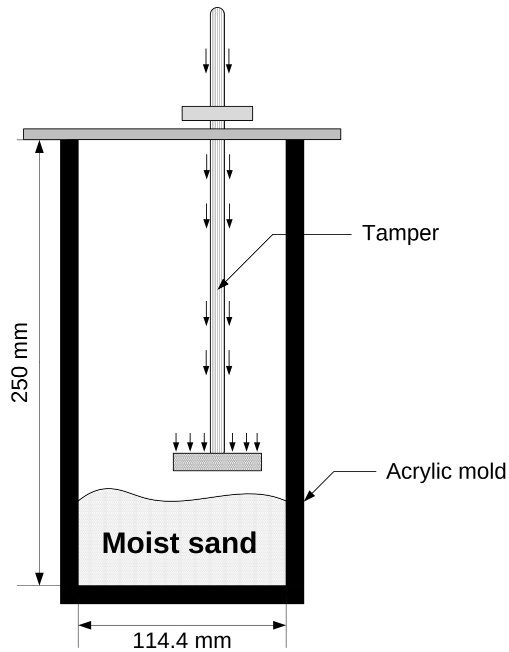

Figure 2: Schematic of the moist tamping specimen preparation method

Materials

Two gradations of Ottawa sand (called “Barco 32” and “Barco 71”) as well as a local silty sand (with a fines content of 11%) from the Boler Mountain (London, Ontario) were used in the experiments of this investigation. The particles of Barco 32 and Barco 71 sands are purely quartz with rounded to subrounded shapes, while the Boler Mountain sand is composed of subrounded to subangular particle shapes with mixed mineralogy of quartz, feldspar and carbonates. Barco 71 sand was mixed with different amounts of quartz silt particles to produce different silty sands and investigate the effect of fines content (FC). Figure 3 shows the gradations of these materials. Table 1 presents the grain density (G_s) of the sand particles as well as their minimum (n_{min}) and maximum (n_{max}) porosities. These properties were determined according to the ASTM standard procedures (ASTM, 2006a, ASTM, 2006c, ASTM, 2006d).

Table 1. Physical properties and index characteristics of the tested sands

Sand	G_s	n_{min}	n_{max}
Barco 32	2.65	0.346	0.444
Barco 71	2.65	0.332	0.451
Boler Mountain	2.65	0.310	0.486

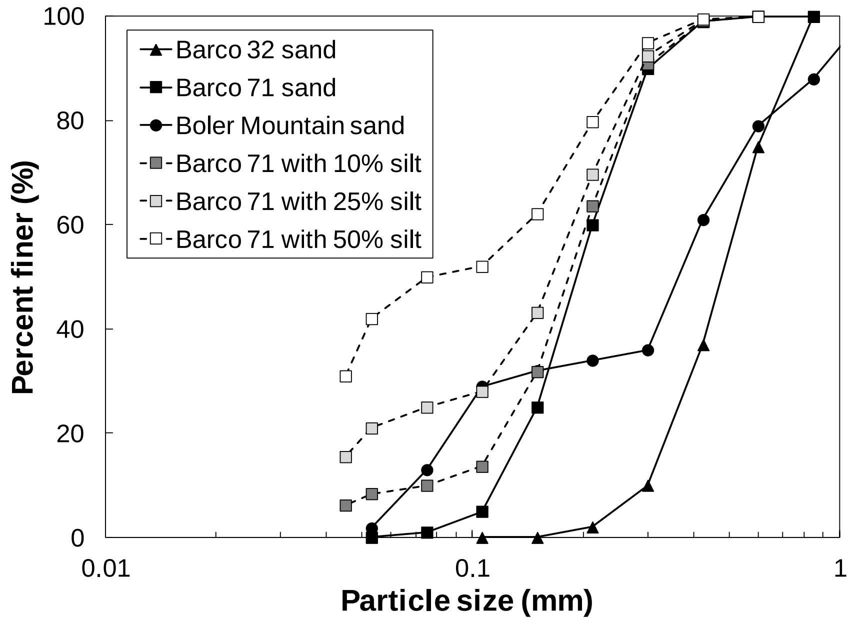

Figure 3: Particle size distributions of the sands used in this study

Electrical resistivity measurement

A portable electrical resistivity probe (Stevens Water Monitoring System Inc, 2007) was used to measure the electrical resistance (*R*) as well as the temperature of the soil water system. The probe consists of four parallel stainless steel electrodes spaced at a center-to-center distance of 13 mm. Each electrode is 55 mm long and 4 mm in diameter with an apex angle of 33^o. Figure 4 shows the schematic shape and dimensions of the probe. The probe introduces a low-frequency (50 Hz) alternating electrical current of known intensity (*I*) into the soil sample at a certain depth through the electrodes, and measures the potential voltage difference (*V*) in the soil adjacent to the electrodes. The low alternating electrical current frequency of 50 Hz minimizes the detrimental effect of polarization of the electrodes. The average electrical resistance of the soil sample around the electrodes is then calculated from Ohm's law ($R = V/I$). These data are transferred to and displayed on a handheld PDA. Soil electrical resistivity (ρ_b), a fundamental soil property, is obtained by multiplying the measured resistance (*R*) by the geometrical factor, *K* of the probe ($\rho_b = K \times R$) which depends on the size and the separation of the electrodes. An average geometrical factor of 0.872 was determined for the probe by calibration with a TetraCon 325 4-electrode conductivity cell in an ionic buffer solution of 3gr/L salt (NaCl) at a measured electrical resistivity of 2.127 ohm.m. All experiments were performed at a controlled laboratory temperature of 20°C and in a non-metallic (acrylic) cylinder as metal could interfere with the measurements. Four successive measurements were then taken for each sample. For each measurement, the electrodes were completely inserted into the soil until the base plate of the probe became flush with the soil and readings were taken until soil resistivity and temperature were stabilized. These measurements were very close which indicated the high level of repeatability of the measurements. The average electrical resistivity measurements of each sample are reported in this paper.

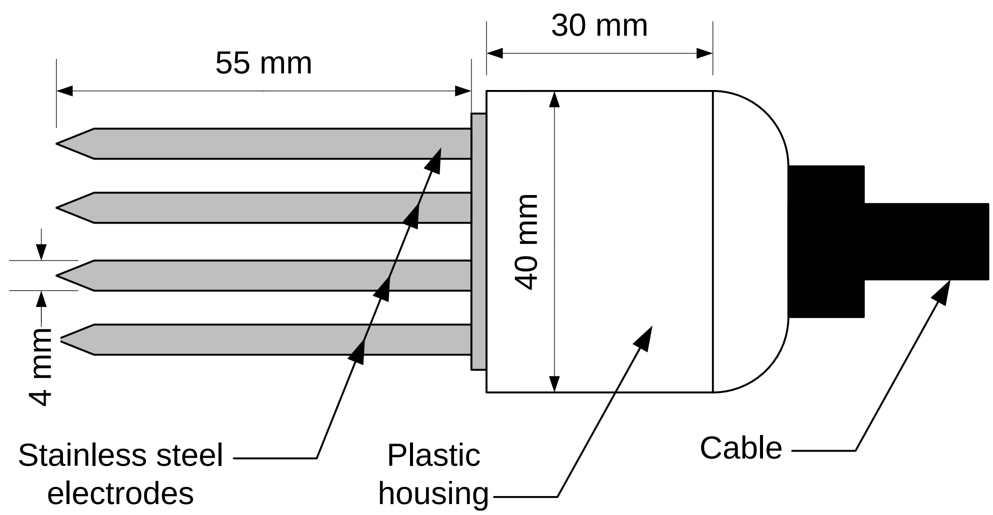

Figure 4: Schematic shape and dimensions of the electrical resistivity probe used in this study

Results and Discussion

The results of the experiments are presented below. For each experiment, sample porosity was determined based on the weight of the soil used for sample preparation and sample volume while ρ_b was measured using the electrical resistivity probe.

Effect of electrolyte concentration

Electrical resistivity of the pore water (ρ_f) depends on the electrolyte concentration as a result of pore water salinity, and thus at a certain porosity the electrical resistance of a saturated cohesionless soil would become a function of the amount of salt in the pore fluid. Figure 5 presents the electrical resistivity of saturated Barco 71 sand samples with different amounts of pore water salinity expressed in grams of salt per 1 liter of distilled water. Based on this figure, salt content of the pore fluid electrolyte has a profound impact on the electrical resistivity of soil as ρ decreases with increasing salt concentration of the pore water.

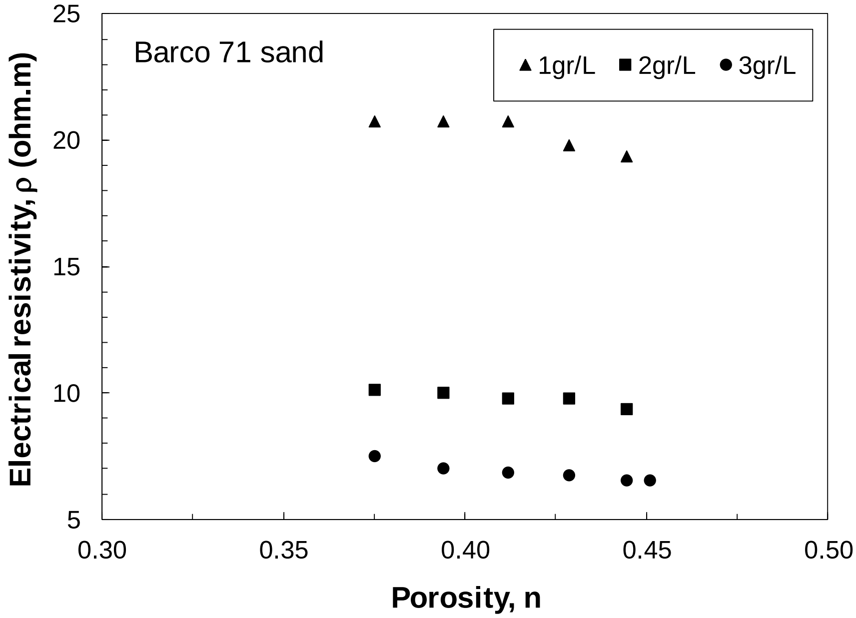

Figure 5: Effect of pore water salinity on electrical resistivity of saturated Barco 71 sand samples

Figure 5 further indicates that soil electrical resistivity is inversely proportional to its porosity. As porosity increases, the electrical resistivity slightly decreases. As this investigation is focused on sands with non-conductive silicate particles, increasing of the electrical conductivity is due to the increase of the conducting pore water volume among the sand particles and the ability of the electrolyte water to conduct electricity, reducing the electrical resistivity of the saturated sand.

Effect of particle size distribution

Figure 6 compares the electrical resistivity of the different sands tested in this study, which clearly indicates increasing soil electrical resistivity with increasing of the amount of fines. Increasing fines content, even at the same porosity, reduces the number and the volume of connections among the pores of a sand and thus the electrical connectivity and conductivity of the pore fluid. Despite differences in particle size distributions (see Fig. 3), the Barco 32 and Barco 71 sands exhibit nearly similar electrical resistivity at FC = 0%, or the Boler Mountain and Barco 71 sands with 10 to 11% fines contents show similar electrical resistivity. Hence, the effect of variations in particle size distribution on the electrical resistivity of sands seems to be secondary to the effect of FC. A similar observation was made by Keller and Frischkecht (1966).

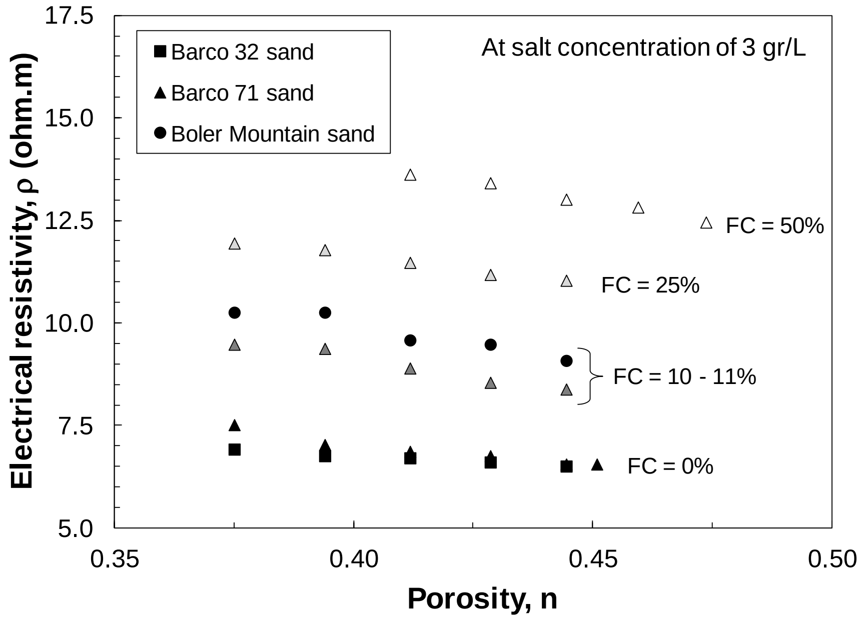

Figure 6: Effect of sand particle size distribution and fines content (FC) on electrical resistivity with a pore water salt concentration of 3 gr/L

Effect of specimen preparation method

In order to investigate the effect of sand fabric on the electrical resistivity of saturated sands, a number of experiments were conducted on Barco 71 sand samples prepared by air and water pluviation methods. These methods resemble sand fabrics formed by natural aeolian and fluvial process (e.g. in rivers and streams), respectively (Oda, et al., 1978, Vaid and Eliadorani, 1998). Air pluviated specimens were prepared by raining sand particles into the cylindrical mold through air. The porosity and density of the samples prepared by air pluviation was varied by changing the free-fall height and thus the depositional velocity of the particles. For preparing very loose samples, sand particles were rained with nearly zero drop height. A similar procedure was used to prepare water pluviated specimens by raining sand particles through water. However, as the particles reach a terminal velocity after a certain drop height in water, lower porosities were produced by tapping the sides of the specimen mold and thus densifying the sand sample. Figure 7 shows the results of these experiments. Electrical resistivity of the samples prepared by the pluviation methods fall nearly on the same trendline, despite the larger porosities of the water pluviated samples. However, the electrical resistivities of the moist tamped samples are slightly greater which is likely because of the comparatively isolated pores of the honeycomb moist tamped sand fabric.

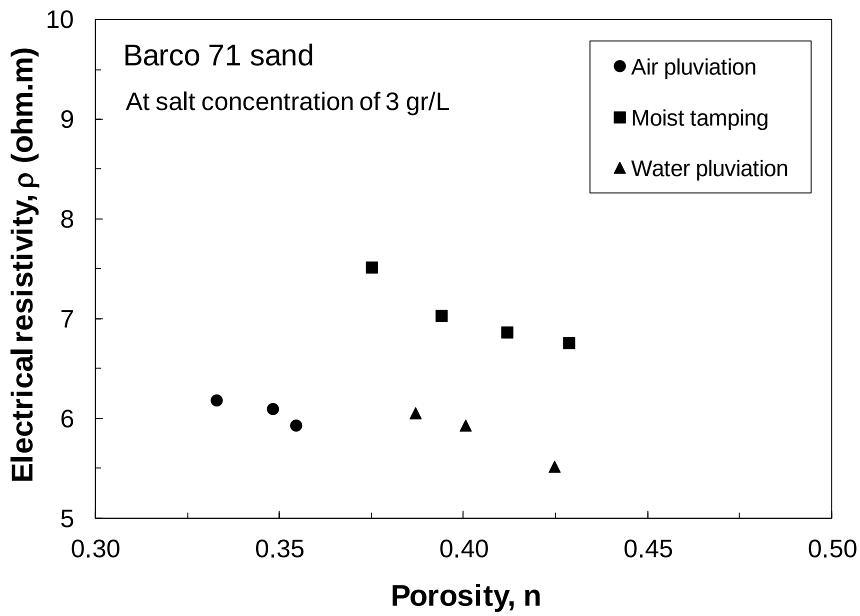

Figure 7: Effect of specimen preparation method on electrical resistivity of Barco 71 sand

Estimation of porosity

In order to develop a practical relationship, the effects of electrolyte salinity and probe geometry are removed by presenting the results in terms of formation factor (*FF*) and porosity (*n*) in Figure 8. Electrical resistivity data for several other sands (platy sand, sand with 1% shell content, rounded sand, and sand and gravel) with different particle size distributions and particle shapes (Arulmoli, et al., 1985, Borner, et al., 1996, Jackson, et al., 1978) are also included in this figure. According to Figure 8, *FF* generally increases with decreasing sand porosity (or increasing density) due to the smaller water saturated pore volume of dense sands. According to these data, variations in gradation, mean particle size, and particle shape have little influence on the trend of data. The most significant changes in *FF* are produced by changes in FC, while the scatter at a certain FC are probably associated to variations in sand gradation and method of sample preparation.

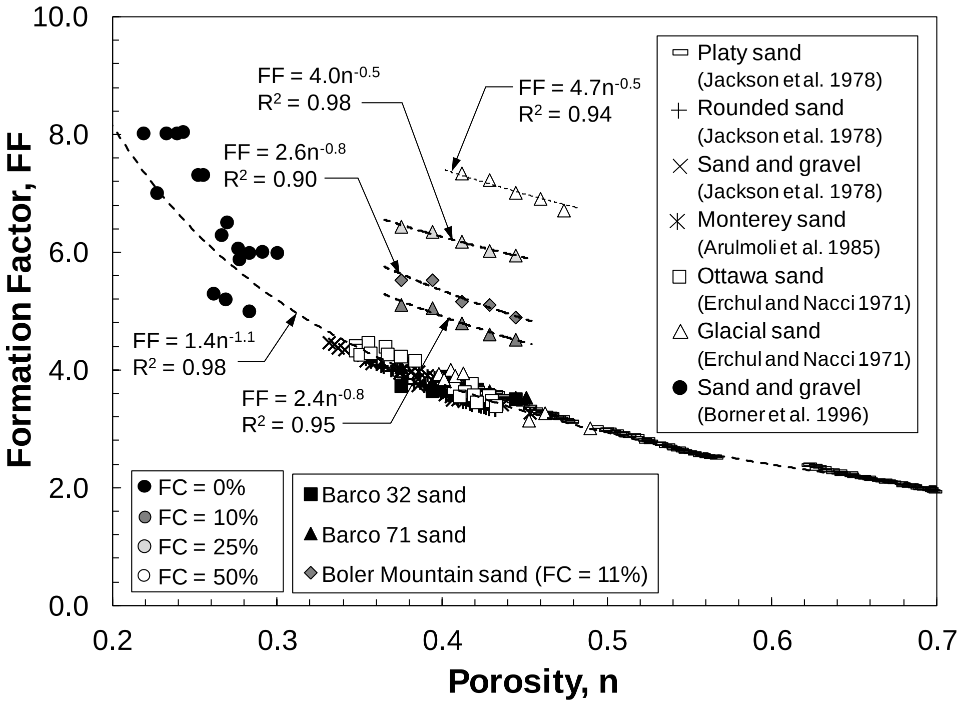

Figure 8: Effect of porosity on *FF* for the cohesionless soils tested in this study as well as for a platy sand, a rounded quartz sand, a quartz sand and gravel mixture (Jackson, et al., 1978) several other sands (Arulmoli, et al., 1985, Borner, et al., 1996, Jackson, et al., 1978)

Data at certain FC are also curve fitted with Equation [1] and the fitting parameters (*a*, *m*) are shown in Figure 8. In contrast to other studies, rather than particle shape (Jackson, et al., 1978) or cementation (Archie, 1942), Figure 8 indicates that the parameters of Equation [1] largely depend on FC. Fine particles increase the tortuosity and thus the length of the path that an electrical current must follow as well as constricting the openness of these flow channels. And therefore FF increases with increasing FC as a result of increasing tortuosity (Lesmes and Friedman, 2005, Schon, 2004). Figure 9 illustrates that coefficient *a*, and the exponent *m* respectively increase and decrease with increasing FC. For sands of this study, the specific relationships of these parameters with FC are also provided in Figure 9. As the experiments of this study were performed at small stress levels (< 5 kPa) the effect of stress level cannot be inferred from these results. However, based on past experimental observations (Hulbert, et al., 1982, Lee, et al., 2008, Lewis, et al., 1988), *FF* varies with stress to the extent that soil porosity is altered by stress. In other words, at a certain porosity stress does not appear to affect *FF*.

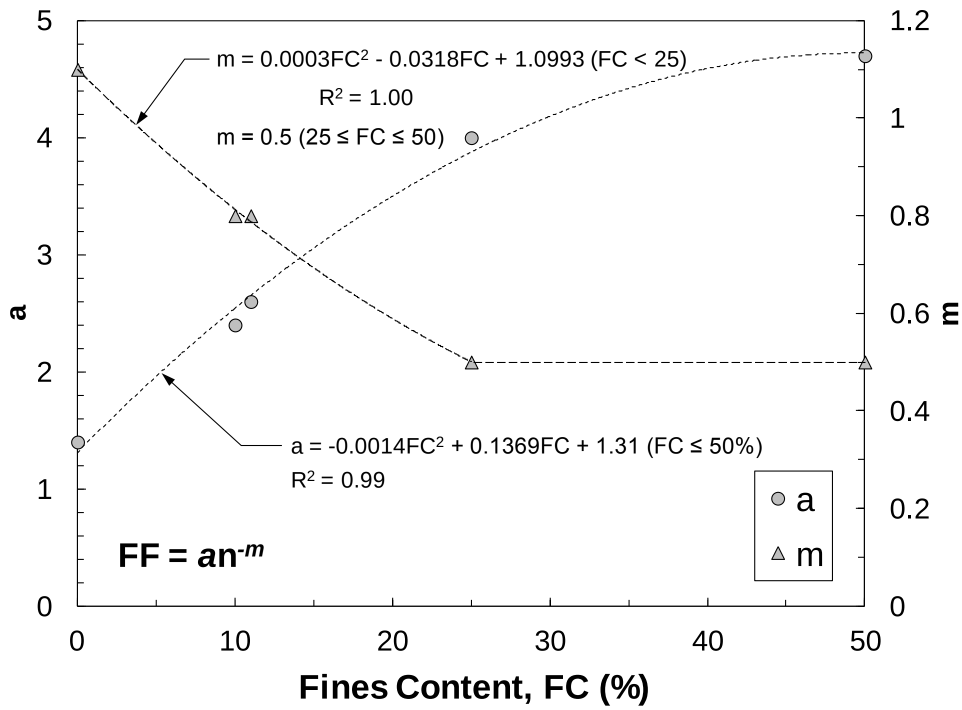

Figure 9: Variations of the parameters of Equation [1] with FC for the sands of this study

Estimation of Hydraulic Conductivity

Besides electrical resistivity, the coefficient of permeability (*k*) of the specimens was obtained by preparing saturated samples (at porosities similar to the electrical resistivity tests) in a constant-head permeameter cell. The permeability of these specimens was then measured following the ASTM D2434 (2006b) standard procedure for constant-head permeability tests. In this method, the sample is subjected to a water flow with a constant pressure head while the rate of flow and therefore *k* are measured. This procedure provides representative values of k that may occur in natural deposits or in embankments. Figure 10 shows unique relationships (similar to Eq. [1]) between the results of these experiments with *FF* as well as those from Jones and Buford (1951) at certain FC. These data show that a higher *FF* would indicate an aquifer with higher permeability and yield. The good relationship between *FF* and permeability is somewhat expected as porosity and permeability are directly related and both electrical current and fluid flow move in tortuous paths through the intergranular pores of a soil. Particularly in sandy soils where there is no interaction between the ionic constituents of the porewater and the matrix solid, the bulk resistivity of a soil-water system would be a function of pore volume tortuousity, and porosity and hence permeability. As illustrated in Figure 10, the addition of fine particles affects the pore sizes and the resulting permeability more significantly than porosity, as permeability is approximately proportional to the square of the pore sizes (Hazen, 1911). With increasing fines content, the porosity exponent increases from 0.03 to 0.14.

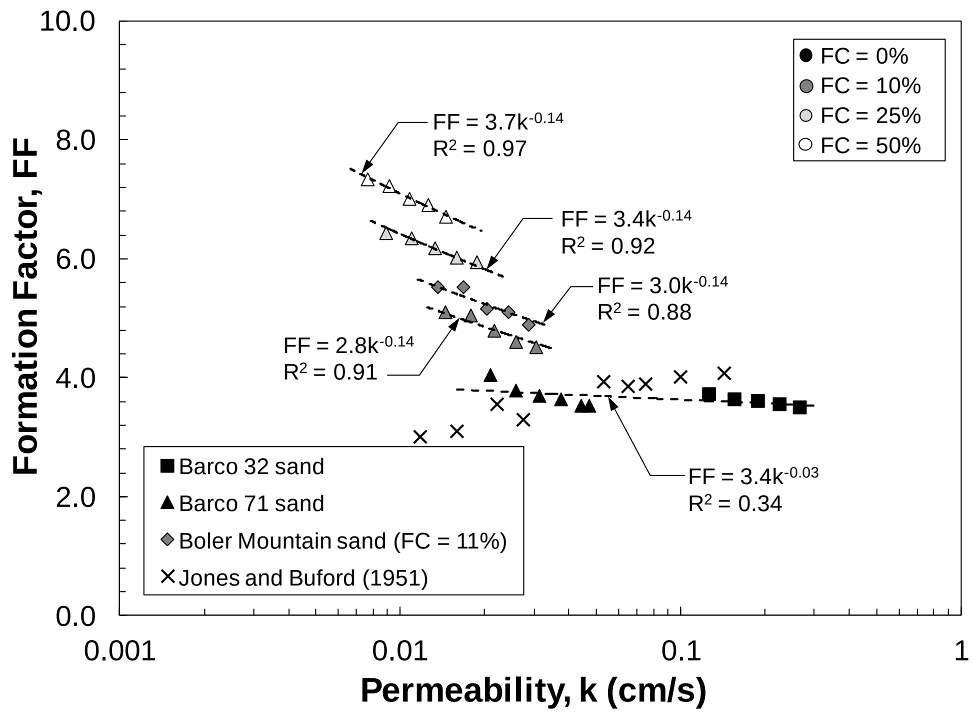

Figure 10: Variations of hydraulic conductivity and *FF* for the cohesionless soils of this study as well as for a sand from Jones and Buford (1951)

A number of studies (Borner, et al., 1996, Pape, et al., 1987) have related hydraulic conductivity to the formation factor and the specific surface area of sediments (S_A). For example, based on a modified form of the Kozeny-Carman's hydraulic conductivity relationship, Pape et al. (1987) suggested the following equation (known as the "PARIS" equation) for predicting hydraulic conductivity:

$$k = \frac{\gamma_w}{\eta_w} \cdot \frac{475}{FFS_A^{3.1}} \qquad \text{Equation [2]}$$

In which, γ_w (= 9.81 kN/m^3) and η_w (=1.002×10^{-6} kPa.s) are the unit weight and dynamic viscosity of water at 20^{o}C. Later, using spectral induced polarization as well as complex electrical resistivity measurements, Borner et al. (1996) found the following proportionality from their laboratory experiments:

$$k \cong \frac{1}{FFS_A^c} \qquad \text{Equation [3]}$$

in which S_A is determined from electrical measurements and the exponent c is in the range of 2.8 to 4.6. Similar to the Kozeny-Carman's equation, the application of Equations (2), and (3) is limited because of the difficulty in determining S_A of sediments which normally requires nitrogen gas adsorption measurements (Hillel, 1980). Although S_A was not measured for the sediments of this study, correlations of Figure 10 suggest a modified form of Equation [3] as below:

$$k = \frac{A}{FF^c} \qquad \text{Equation [4]}$$

In which, the coefficient A could include S_A of the corresponding sand. The difference with Equations (2) and (3) results from the exponent ("c") applied to FF.Note that the plots of Figures 8 to 10 as well as the findings of this paper are only applicable to saturated cohesionless soils with non-conductive particles. The result might be inapplicable for clayey, organic, or cemented soils as the surface conduction of clay particles could dominate the electrical resistivity of a clayey soil (Erickson and Jarrard, 1998).

Site specific calibration is recommended for using electrical resistivity measurements for estimating sand porosity, yet in the absence of such data the correlations presented in Figures 8 and 9 can be employed to determine the in-situ density and seepage characteristics of sands. Following the determination of in-situ porosity, laboratory sand specimens can be prepared at representative porosities for the estimation of the in-situ strength of sandy soils.

Since changes in electrical resistivity result from changes in pore water volume, the application of this method would require saturated soil conditions. Determination of the formation factor also requires a separate measurement of the pore water resistivity. Offshore and surficial seabed sediments would thus be the ideal conditions for the application of this method as the salinity of the pore waters would vary little from that of the seawater (Siever, et al., 1965). The in-situ resistivity of pore water (ρ_f) – which is needed to calculate *FF* - can be readily measured just before the probe penetrates into the sediment without taking water samples. This can provide relatively quick and inexpensive measurements of in-situ porosity and permeability of cohesionless sediments.

Conclusions

The results of this study show that the electrical resistivity of cohesionless soils decreases with increasing pore water salinity, and porosity while soil fabric, particle size distribution and shape of the particles have negligible effects on electrical resistivity. However, the amount of silt particles (between 0.002 to 0.075 mm, according to the Unified Soil Classification System) has a profound impact on the resistivity of a saturated cohesionless soil to an electrical current. Accordingly, a number of correlations are developed between electrical resistivity, and porosity and hydraulic conductivity of cohesionless soils for certain fines contents. These results suggest that electrical resistivity can provide a useful measurement for estimating the porosity and permeability of cohesionless soils through Archie's law. Measurement of porosity and in-situ density of cohesionless soils is essential for predicting their behavior under shear loading. However this could be difficult due to sample disturbance and the inherent variability of in-situ cohesionless soils. In the absence of site specific data, the relationships developed in this study could be employed to determine the in-situ density and hydraulic conductivity of saturated cohesionless soils indirectly from electrical resistivity measurements.

References

Abu-Hassanein, Z. C., Benson, C. H., and Blotz, L. R. (1996). "Electrical resistivity of compacted clays." *Journal of Geotechnical Engineering, ASCE*, 122(5), 397 - 406.

Archie, G. E. (1942). "The electrical resistivity log as an aid in determining some reservoir characteristics." *Transactions of the American Institute of Mining and Metallurgical Engineers Petroleum Division*, 146(1), 54 - 62.

Arulmoli, K., Arulanandan, K., and Seed, H. B. (1985). "New method for evaluating liquefaction potential." *Journal of Geotechnical Engineering*, 111(1), 95-114.

ASTM (2006a). "Standard D854: Standard Test Methods for Specific Gravity of Soil Solids by Water Pycnometer." *Annual Book of ASTM Standards*, ASTM International, West Conshohocken, PA, 100 - 106.

ASTM (2006b). "Standard D2434: Standard Test Method for Permeability of Granular Soils (Constant Head)." *Annual Book of ASTM Standards*, ASTM International, West Conshohocken, PA.

ASTM (2006c). "Standard D4253: Standard test methods for maximum index density and unit weight of soils using a vibratory table." *Annual Book of ASTM Standards*, ASTM International, West Conshohocken, PA.

ASTM (2006d). "Standard D4254: Standard test methods for minimum index density and unit weight of soils and calculation of relative density." *Annual Book of ASTM Standards,* ASTM International, West Conshohocken, PA.

Atkins, E. R., Jr., and Smith, G. H. (1961). "The significance of particle shape in formation factor-porosity relationships." *Journal of Petroleum Technology*, 13(3), 285 - 291.

Barnes, B. B., Corwin, R. F., Beyer, J. H., and Hilden- brand, T. G. (1972). "Geologic prediction: developing tools and techniques for the geophysical identification and classification of sea-floor sediments.", U.S. Dept. Commerce, 163.

Borner, F. D., Schopper, J. R., and Weller, A. (1996). "Evaluation of transport and storage properties in the soil and groundwater zone from induced polarization measurements." *Geophysical Prospecting*, 44, 583 - 601.

Boyce, R. E. (1968). "Electrical resistivity of modern marine sediments from the Bering Sea. ." *Journal of Geophysical Research*, 73(14), 4759 - 4766.

Bryson, L. S., and Bathe, A. (2009). "Determination of Selected Geotechnical Properties of Soil Using Electrical Conductivity Testing." *Geotech Test J*, 32(3), 252-261.

Campanella, R. G., and Weemees, I. (1990). "Development and use of an electrical resistivity cone for groundwater contamination studies." *Canadian Geotechnical Journal*, 27(5), 557 - 567.

Carothers, J. E., and Porter, C. R. (1971). "Formation factor - porosity relation derived from well log data." *The Log Analyst*, 12(1), 16 - 26.

Cho, G. C., Lee, J. S., and Santamarina, J. C. (2004). "Spatial variability in soils: High resolution assessment with electrical needle probe." *J Geotech Geoenviron*, 130(8), 843-850.

Erchul, R. A., and Nacci, V. A. (1971). "The use of marine electrical resistivity measurements to predict porosity of marine sediments." *Proc., Int. Symp on Engineering properties of sea-floor soils and the geophysical identification*, 296 - 308.

Erickson, S. N., and Jarrard, R. D. (1998). "Porosity/formation-factor relationships for siliciclastic sediments from Amazon Fan." *Geophysical Research Letters*, 25(13), 2309 - 2312.

Fourie, A. B., Blight, G. E., and Papageorgiou, G. (2001). "Static liquefaction as a possible explanation for the Merriespruit tailings dam failure." *Canadian Geotechnical Journal*, 38(4), 707-719.

Hazen, A. (1911). "Discussion of 'Dams on Sand Foundations' by A. C. Koenig." *ASCE Transactions*, 73, 199.

Hillel, D. (1980). *Fundamentals of soil physics.*, Academic Press, New York.

Hulbert, M. H., Bennett, R. H., and Lambert, D. N. (1982). "Seabed geotechnical parameters from electrical conductivity measurements." *Geo-Marine Letters*, 2, 219 - 222.

Jackson, P. D., Taylor-Smith, D., and Stanford, P. N. (1978). "Resistivity-porosity-particle shape relationships for marine sands." *Geophysics*, 43(6), 1250 - 1268.

Jones, P. H., and Buford, T. B. (1951). "Electric logging applied to ground-water exploration." *Geophysics*, 16(1), 115 - 139.

Keaton, J. R., Wartman, J., Anderson, S. A., Benoît, J., de La Chapelle, J., Gilbert, R., and Montgomery, D. R. (2014). "The 22 March 2014 Oso Landslide, Snohomish County, Washington." *Turning Disaster into Knowledge*, Geotechnical Extreme Events Reconnaissance, 172 pp.

Keller, G. V., and Frischknecht, F. C. (1966). *Electrical methods in geophysical prospecting.*, Pergamon Press, New York.

Kermabon, A. J., Gehin, C., and P., B. (1969). "A deep-sea electrical resistivity probe for measuring porosity and density of unconsolidated sediments." *Geophysics*, 34, 534 - 571.

Kim, J. H., Yoon, H. K., and Lee, J. S. (2011). "Void Ratio Estimation of Soft Soils Using Electrical Resistivity Cone Probe." *J Geotech Geoenviron*, 137(1), 86-93.

Kosinski, W. K., and Kelly, W. E. (1981). "Geoelectric soundings for predicting acquifer properties." *Ground Water*, 19(2), 163 - 171.

Ladd, R. S. (1978). "Preparing test specimens using undercompaction." *Geotechnical Testing Journal, ASTM*, 1(1), 16 - 23.

Lee, C., Lee, J.-S., Lee, W., and Cho, T.-H. (2008). "Experiment setup for shear wave and electrical resistance measurements in an oedometer." *Geotechnical Testing Journal, ASTM*, 31(21), 149 - 156.

Lesmes, D. P., and Friedman, S. P. (2005). "Relationships between the electrical and hydrogeological properties of rocks and soils." *Hydrogeophysics*, Y. Rubin, and S. S. Hubbard, eds., Springer, Dordrecht, Netherlands, 87 - 128.

Lewis, M. G., Sharma, M. M., and Dunlap, H. F. (1988). "Wettability and stress effect on saturation and cementation exponents." *Transactions of the SPWLA Twenty-Ninth Annual Logging Symposium*, Society of Professional Well Log Analysts, San Antonio, Texas.

Oda, M., Koishikawa, I., and Higuchi, T. (1978). "Experimental study of anisotropic shear strength of sand by plane strain test." *Soils and Foundation*, 18(1), 25-38.

Pape, H., Riepe, L., and Schopper, J. R. (1987). "Theory of self-similar network structures in sedimentary and igneous rocks and their investigation with microscopical and physical methods. ." *Journal of Microscopy*, 148, 127-147.

Sadrekarimi, A. (2009). "Development of a new ring shear apparatus for investigating the critical state of sands."Ph.D. thesis, University of Illinois, Urbana-Champaign, Urbana, Illinois.

Sadrekarimi, A. (2013). "Influence of state and compressibility on liquefied strength of sands." *Canadian Geotechnical Journal*, 50(10), 1067 - 1076.

Salem, H. S., and Chilingarian, G. V. (1999). "The cementation factor of Archie's equation for shaly sandstone reservoirs." *Journal of Petroleum Science and Engineering*, 23, 83 - 93.

Schon, J. H. (2004). "Physical properties of rocks: fundamentals and principles of petrophysics." *Handbook of Geophysical Exploration: Seismic Exploration*, K. Helbig, and S. Treitel, eds., Elsevier Ltd., Oxford, UK, 379 - 479.

Siever, R., Beck, K. C., and Berner, R. A. (1965). "Composition of interstitial waters of modern sediments." *Journal of Geology*, 73, 39 - 73.

Stevens Water Monitoring System Inc (2007). "Comprehensive Stevens Hydra Probe Users Manual." S. W. M. S. Inc., ed., Stevens® Water Monitoring System, Inc., Portland, OR.

Taylor-Smith, D. (1971). "Acoustic and electric techniques for sea-floor sediment identification." *Proc., Proceedings of the International Symposium on Engineering Properties of the Sea-Floor and their Geophysical Identification*, 253 - 267.

Urish, D. W. (1981). "Electrical resistivity-conductivity relationships in glacial outwash aquifers." *Water Resources Research*, 17(5), 1401 - 1408.

Vaid, Y. P., and Eliadorani, A. (1998). "Instability and liquefaction of granular soils under undrained and partially drained states." *Canadian Geotechnical Journal*, 35(6), 1053-1062.

Wheatcroft, R. A. (2002). "In-situ measurements of near-surface porosity in shallow-water marine sands." *IEEE Journal of Oceanic Engineering*, 27(3), 561 - 570.

Winsauer, W. O., Shearin, H. M., Masson, P. H., and Williams, M. (1952). "Resistivity of brinesaturated sands in relation to pore geometry." *Bulletin of the American American Association of Petroleum Geologists*, 36, 253 - 257.